2011

Large magnetoelectric effect in ferroelectric/piezomagnetic heterostructures

Pavel Lukashev
University of Nebraska-Lincoln, pavel.lukashev@uni.edu

Kirill D. Belashchenko
University of Nebraska-Lincoln, belashchenko@unl.edu

Renat F. Sabirianov
University of Nebraska at Omaha, rsabirianov@mail.unomaha.edu

Large magnetoelectric effect in ferroelectric/piezomagnetic heterostructures

Pavel Lukashev,[1,2] Kirill D. Belashchenko,[1,2] and Renat F. Sabirianov[3,2]
[1]*Department of Physics and Astronomy, University of Nebraska-Lincoln, Lincoln, Nebraska, 68588-0299, USA*
[2]*Nebraska Center for Materials and Nanoscience, University of Nebraska-Lincoln, Lincoln, Nebraska, 68588-0299, USA*
[3]*Department of Physics, University of Nebraska at Omaha, Omaha, Nebraska 68182-0266, USA*
(Received 12 August 2011; published 17 October 2011)

We present results of the first-principles calculations on the large magnetoelectric effect in ferroelectric/piezomagnetic multilayers. We consider thin-film layered heterostructures of typical ferroelectrics, such as $PbTiO_3$, with piezomagnetic (PzM) Mn-based antiperovskites, such as Mn_3GaN. The atomic displacements induced by the FE polarization as well as mechanical stress at the interface break the triangular magnetic symmetry of the PzM phase producing net magnetization in the system. The induced magnetization can be controlled by changing the direction of polarization in the ferroelectric phase. Our calculations show that reversal of the polarization results in change of the net magnetization in the system by more than 50%.

DOI: 10.1103/PhysRevB.84.134420 PACS number(s): 75.50.−y, 75.80.+q

I. INTRODUCTION

The control of the magnetic properties of complex materials by external electric field and electrically driven switching phenomena have attracted significant interest because of their potential applications, which may prove to be faster and more energy efficient than the current memory or electronics technology. Materials, which possess ferroelectric (FE) polarization and magnetization, are called multiferroic and the coupling between these two order parameters constitutes a magnetoelectric (ME) effect.[1] Compared to bulk multiferroics,[2] only a few of which are known, heterostructures made of FE and ferromagnetic (FM) components show stronger ME coupling.[3] In most of the proposed systems, ME coupling in the heterostructures is strain mediated, in contrast to the mechanism related to displacement of magnetic atoms in the bulk multiferroics. Recently, novel mechanisms were established that lead to ME coupling. At ferromagnet/insulator interfaces the ME effect may originate from purely electronic mechanisms. It was predicted that atomic displacements at the FM/FE interface caused by FE switching change the overlap between atomic orbitals at the interface, which in turn affects the interface magnetization.[4,5] Recently, it was demonstrated that ME effect can be induced by free carriers.[6] In this case, due to spin-dependent screening,[7] an applied electric field produces an accumulation of spin-polarized electrons or holes at the metal-insulator interface resulting in a change of the interface magnetization[8] and the exchange splitting.[9–11]

In this paper, we explore ME phenomena in layered FE/PzM heterostructures based on antiperovskite materials, which have zero net magnetization in the ground state. In particular, we consider a thin-film layered heterostructure of Mn_3GaN with ferroelectric $PbTiO_3$. We study possible mechanisms of the magnetization induction in this system, such as atomic displacements caused by FE polarization and surface strain due to lattice mismatch, which may break the magnetic symmetry of the Mn_3GaN, producing net magnetization in the system. We also consider the possibility of controlling the induced magnetization in PzM phase by switching the direction of the polarization in FE phase.

II. Mn-BASED ANTIPEROVSKITES

Antiperovskite compounds belong to the same crystallographic space group as regular perovskites. However, in antiperovskites the 3c sites are not occupied by oxygen but by transition-metal atoms like Mn, forming the corresponding cages of octahedral symmetry as shown in Fig. 1. These materials show a variety of magnetic structures and phase transitions. Many interesting properties of antiperovskites have been reported, such as Invar effect or even negative thermal expansion,[12] near-zero temperature coefficient of resistance,[13] a giant magnetoresistance,[14] piezomagnetic,[15] and flexomagnetic[16] effects. The magnetic ground state of Mn_3GaN is shown in Fig. 1. This is the noncollinear Γ^{5g} structure (in the classification of Bertaut *et al.*)[17] with the local magnetic moments on the (111) plane forming clockwise or counterclockwise configurations, compensating each other. As a result, in the ground state, Mn_3GaN has zero net magnetization. Yet, our recent study[15] shows that these compounds exhibit a linear PzM effect, in particular, appearance of the net magnetization upon application of in-plane biaxial strain. The PzM effect is due to the rotation of the local magnetic moments of the Mn atoms from their equilibrium directions. Upon rotation the moments in the (111) plane become inequivalent.

The threefold-symmetry magnetic structure in Mn_3GaN is due to the negative exchange interaction on the frustrated (111) planes, which are similar to kagome lattices. The interfaces of such lattice with perovskite systems should alter their magnetic structure because the exchange interactions of the interface atoms with the inner layers of Mn_3GaN will be modified, and exchange interactions between interfacial Mn atoms will also change. This removes the threefold symmetry in the system and magnetization is expected to be induced. For example, if we consider three antiferromagnetically coupled Mn atoms arranged on the corners of equilateral triangle, the lowest-energy state corresponds to the triangular magnetic structure, i.e., the angles between directions of the spin moments are 120°. However, if the exchange coupling between one of the spin pairs is altered, then the lowest-energy state will have net magnetization because the angle between spin moments will change. The larger modification of exchange

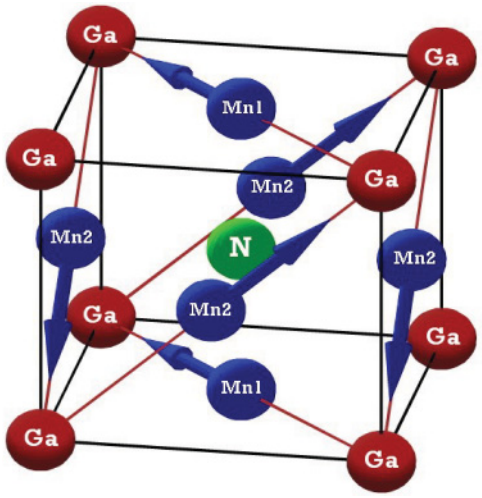

FIG. 1. (Color online) Mn_3GaN unit cell: noncollinear Γ^{5g} magnetic ground-state structure. Arrows represent local magnetic moments of Mn atoms.

parameters at the interface corresponds to the larger value of the induced magnetization. Therefore the rotation of interfacial spin moments changes the overall magnetic structure of the film. At two inequivalent interfaces, different magnetizations are expected to be induced. The change in the exchange coupling between Mn sites at the interface due to the atomic displacements in FE phase is expected to be large because of the generally strong dependence of exchange coupling on interactomic distance. Details of the exchange interaction mechanism in Mn_3GaN are provided in Ref. 16.

Since the PzM effect is linear in Mn_3GaN, the magnetization in the PzM/FE heterostructures should be induced without need for the external magnetic field. This is the main difference between the system considered in this paper and FE/magnetostrictive heterostructures.

III. COMPUTATIONAL MODEL AND METHODS

We perform our calculations using the projector augmented wave (PAW) method,[18] implementation of PAW in Vienna *ab initio* simulation package (VASP) code[19] within a local density approximation (LDA) of the density functional theory (DFT). We use $8 \times 8 \times 1$ k-point sampling and the Methfessel-Paxton integration method[20] for the heterostructure and tetrahedron method for $PbTiO_3$ and Mn_3GaN calculations. We form a stoichiometric heterostructure consisting of four unit cells of $PbTiO_3$ and four unit cells of Mn_3GaN. The termination interface is assumed to be PbO/GaMn and TiO_2/Mn_2N, which corresponds to the electrostatically optimal configuration, i.e., Mn sites neighbor oxygen, while Pb neighbors Ga. Other terminations (PbO/Mn_2N and TiO_2/GaMn) result in strong tetragonal distortion due to atomic charge configuration at the surface.

We choose LDA to treat the exchange and correlation energy of the electrons following earlier reports[21–24] that Perdew-Burke-Ernzerhof (PBE) generalized gradient approximation (GGA)[25] poorly describes FE systems such as $PbTiO_3$ by largely overestimating the c/a ratio and the FE polarization. But for the Mn_3GaN, the LDA fails to correctly describe the magnetic ground state. This problem is solved by on-site replacement of the L(S)DA with the strong intraatomic Hartree-Fock like interaction, a method known as L(S)DA+U. We use the rotationally invariant LSDA+U[26] and the effective on-site Coulomb interaction parameter (U) for Mn atoms of 2 eV. This results in a correct description of the magnetic ground state of Mn_3GaN.

We performed the structural optimization for the perovskite $PbTiO_3$ with the following results: the in-plane lattice constant $a = 3.870$ Å, the c/a ratio is 1.037, and the out-of-plane FE displacements are 0.26 Å between Ti and O atoms and 0.34 Å between Pb and O atoms.[27]

The calculated lattice constant of Mn_3GaN is 3.86 Å,[15] which results in only 0.5% lattice mismatch at the FE/PzM interface. We performed optimization of the heterostructure lattice parameters as follows: (1) we set the in-plane lattice constant to 3.87 Å, (2) the initial FE displacements are chosen from the ground-state values and are always kept fixed in the two "noninterfacial" unit cells of $PbTiO_3$ to preserve the bulk-like FE polarization in the system, and (3) we perform ionic relaxations at different c/a ratios and find the optimal values for both directions of FE polarization. The value of the in-plane lattice constant of 3.87 Å is very close (only ~0.5% larger) to the ground-state lattice constant of the Mn_3GaN, therefore we expect that the magnetic reconstruction on the interface will be mostly due to the FE out-of-plane displacements, not the in-plane strain, hence manifesting the stronger ME coupling. We call polarization right if Ti and Pb atoms are shifted to the right relative to the O atoms as shown on the Fig. 2(a). We call the opposite polarization left [see Fig. 2(b)].

IV. RESULTS

The results of the heterostructure lattice optimization are summarized in Table I. Figure 2 shows the $PbTiO_3/Mn_3GaN$ heterostructure after ionic relaxation for (a) right **P** and (b) left **P**. Figure 3 shows the interatomic distances at the PbO/GaMn and TiO_2/Mn_2N interfaces after relaxation as well as formal valence of the elements for (a) right **P** and (b) left **P**. These two figures show that while noninterfacial cells have interatomic bond distances similar to the bulk values in the parent compound, yet at the same time, there are substantial atomic displacements in interfacial TiO_2 and PbO planes. These displacements also alter the magnetic state of Mn_3GaN substantially. While the bulk antiperovskite has zero

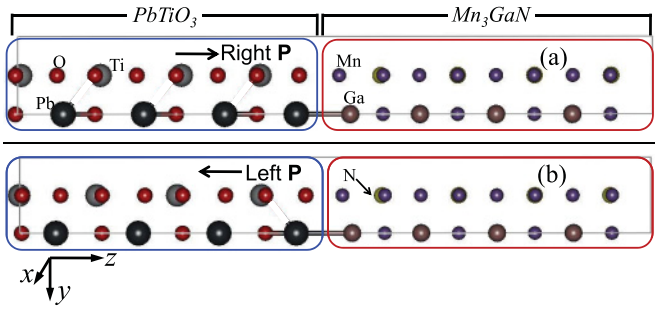

FIG. 2. (Color online) $Mn_{12}Ga_4N_4/Pb_4Ti_4O_{12}$ heterostructure after ionic relaxation: (a) right polarization and (b) left polarization.

TABLE I. Lattice parameters for the heterostructure with left **P** (column 2), right **P** (column 3), $PbTiO_3$ (column 4), and Mn_3GaN (column 5).

	left **P**	right **P**	$PbTiO_3$	Mn_3GaN
a	3.87	3.87	3.870	3.86
c/a	8.32	8.22	1.037	1.00
Ti-O displ.	0.26	−0.26	0.26	N/A
Pb-O displ.	0.34	−0.34	0.34	N/A

net magnetization, the total magnetic moment in the 40-atom cell after relaxation is $\sim 1.63\mu_B$ for the right and $\sim 1.06\mu_B$ for the left **P**. Thus, switching the polarization sign results in change of the induced magnetization by more than 50%, in a clear manifestation of the large magnetoelectric coupling. The induced magnetization is mainly due to the change in the magnetic structure at the interfaces. This is shown on the Fig. 4, which demonstrated the distribution of the induced magnetic moments per Mn_3GaN cell for left **P** (green) and right **P** (blue). The numbering of the unit cells is as follows: *"1"* corresponds to the Mn_3GaN unit cell at the PbO/GaMn interface, *"4"* corresponds to the Mn_3GaN unit cell at the TiO_2/Mn_2N interface, *"2"* and *"3"* correspond to the noninterfacial Mn_3GaN unit cells. The noninterfacial cells for the case of left **P** mainly keep the bulk magnetic structure, which results in their induced magnetization being small. At the same time, the interfacial cells break their magnetic symmetry due to strong structural distortion, which results in large induced magnetic moment. For the right **P**, the distribution of the induced magnetization per cells is different. In particular, there is large magnetization in two unit cells at the TiO_2/Mn_2N and much smaller magnetization at the PbO/GaMn interface. Tables II and III present magnetic moments per Mn_3GaN unit cell resolved in Cartesian coordinates for right and left **P** correspondingly. The numbering of the cells is consistent with the one on the Fig. 4. We can see from Tables II and III that one more difference in the magnetic moment distribution for right and left **P** is that the z component (see Fig. 2) of the induced magnetization is substantially larger for the former than for the latter.

Table IV summarizes values of the Mn magnetic moments for bulk Mn_3GaN[15] as well as for PzM/FE heterostructure with

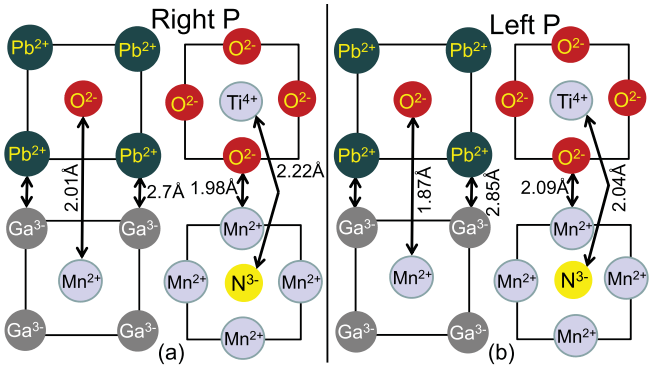

FIG. 3. (Color online) Formal valence of the elements and interatomic distances at the PbO/GaMn and TiO_2/Mn_2N interfaces after relaxation.

TABLE II. Right polarization: magnetic moments per Mn_3GaN unit cell resolved in Cartesian coordinates. Net magnetization in 40-atom cell is $1.63\mu_B$ ($M_x = -1.188\mu_B$, $M_y = -1.074\mu_B$, and $M_z = 0.336\mu_B$).

Mn_3GaN cell	Magn-x	Magn-y	Magn-z	Magn-total
1	−1.126	−1.605	1.494	2.465
2	0.550	1.243	−1.611	2.108
3	−0.148	−0.252	0.461	0.546
4	−0.261	−0.192	0.051	0.328

left and right **P**. There is also induced magnetic moment on Ti and O atoms (not shown in Table IV) but it is quite small. The largest induced magnetic moment on Ti is on the interfaces. In the case of left **P**, there is an induced magnetic moment on the Ti atom of 0.1 μ_B at the TiO_2/Mn_2N interface, while for the right **P** there is an induced magnetic moment of 0.07 μ_B on the Ti atom at the PbO/GaMn interface. The induced magnetic moments on O atoms are even smaller. The values shown in Table IV for the bulk Mn_3GaN reflect orientation of the magnetic moments in the (111) plane, while the initial (before relaxation) moments for the heterostructre were chosen in the (001) plane. Because spin-orbit interactions are not included, the easy axis can be chosen arbitrarily, and, for computational convenience, was taken along (001) axis in the heterostructure calculations. One can see from Table IV that while at the PbO/GaMn interface the in-plane projection of the induced magnetization stays essentially the same upon reversal of FE polarization, yet on the TiO_2/Mn_2N interface it reverses its direction upon reversal of the polarization (schematically shown by the black arrow on the Fig. 4). Indeed, by taking the sum of the components for the local magnetic moments in the *4*th unit cell we see that the resultant induced magnetization on the interface for the left **P** is along (1,1,0) while for the right **P** along (−1,−1,0) direction. Same is true for the *3*rd but not for the *1*st and *2*nd unit cells. This reversal of the magnetization at the interface is one of the mechanisms behind the large ME coupling in the system. The other is the large out-of-plane induced magnetization in the *1*st and *2*nd unit cells for the right **P**. We also emphasize here that since the main contribution to the induced magnetization comes from the interfacial unit cells, we do not expect that increasing the thickness of Mn_3GaN will considerably alter the induced magnetization in the system, i.e., the noninterfacial unit cells of the thicker Mn_3GaN film should have vanishingly small net magnetization.

TABLE III. Left polarization: magnetic moments per Mn_3GaN unit cell resolved in Cartesian coordinates. Net magnetization in 40-atom cell is $1.06\mu_B$ ($M_x = -0.821\mu_B$, $M_y = -0.579\mu_B$, and $M_z = 0.337\mu_B$).

Mn_3GaN cell	Magn-x	Magn-y	Magn-z	Magn-total
1	−2.333	−2.161	0.529	3.224
2	0.153	0.162	−0.180	0.286
3	0.157	0.177	−0.028	0.238
4	1.192	1.187	0.002	1.682

TABLE IV. Local magnetic moments of Mn atoms for three different configurations: (a) bulk Mn_3GaN, (b) PzM/FE heterostructure with left **P**, and (c) right **P**. Numbers in the first column correspond to the four unit cells of Mn_3GaN in the stacking direction, i.e., *1* corresponds to the Mn_3GaN unit cell at the PbO/MnGa interface, *2* to the next Mn_3GaN unit cell, etc. Numbers in the second column correspond to the three Mn atoms in the unit cell, i.e., *1* is the Mn atoms in the MnGa plane, while *2* and *3* are the Mn atoms in the Mn_2N plane.

		bulk			left			right		
		x	y	z	x	y	z	x	y	z
	1	1.73	1.73	0	0.00	−0.22	0.03	1.95	2.96	1.73
1	2	−1.73	0	−1.73	0.43	−2.89	0.32	−2.05	−1.95	0.24
	3	0	−1.73	1.73	−2.76	0.95	0.18	−1.03	−2.61	−0.47
	1	1.73	1.73	0	2.19	2.17	−0.26	2.03	2.26	0.50
2	2	−1.73	0	−1.73	0.92	−2.97	0.07	−2.72	1.27	−0.54
	3	0	−1.73	1.73	−2.95	0.96	0.01	1.24	−2.28	−1.57
	1	1.73	1.73	0	2.19	2.20	−0.07	2.11	2.00	0.21
3	2	−1.73	0	−1.73	0.94	−2.97	0.05	0.73	−2.93	0.44
	3	0	−1.73	1.73	−2.97	0.94	−0.01	−2.99	0.68	−0.18
	1	1.73	1.73	0	2.23	2.20	0.01	2.14	2.12	0.06
4	2	−1.73	0	−1.73	1.71	−2.77	0.03	0.85	−3.28	0.04
	3	0	−1.73	1.73	−2.74	1.76	−0.04	−3.25	0.97	−0.05

The local magnetic moment of Mn at the PbO/GaMn interface is strongly reduced when FE polarization points left. This is the reason why in case of the left **P**, the interfacial unit cell of Mn_3GaN (at the PbO/GaMn interface) has large induced magnetization (the other two Mn local magnetic moments are left uncompensated). The strong reduction of the local magnetic moment on Mn atom at the PbO/GaMn interface in the case of the left **P** is mainly due to proximity of oxygen. The interatomic Mn-O distance in this case is 1.87 Å, which is considerably lower than that in the case of the right **P** (2.01 Å) as can be seen in Fig. 3. The sharp decrease in Mn-O distance is associated with the increased hybridization of Mn and O states and as a result in strong suppression of Mn magnetic moment.

V. ELECTRONIC STRUCTURE

To get further insight into the mechanism behind the large ME effect in the considered system, we turn our attention to the electronic structure analysis. Figure 5 shows calculated densities of states (DOS) for the ground-state bulk Mn_3GaN (top panel) and $PbTiO_3$ (bottom panel). As expected, the former is metallic while the latter is insulating with a wide band gap of ∼1.5 eV.

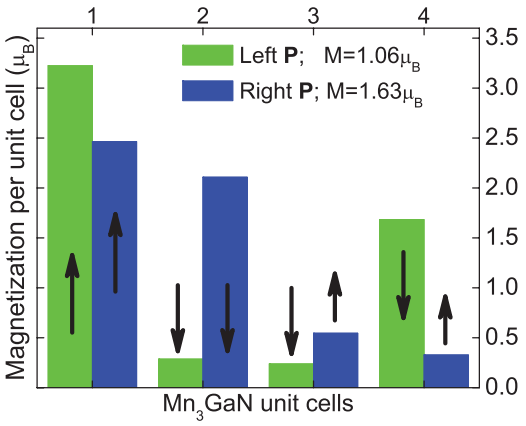

FIG. 4. (Color online) Distribution of the net magnetic moment per Mn_3GaN unit cell for left **P** (green) and right **P** (blue). Black arrows show the (110) direction of the in-plane projection of the magnetization in the unit cell.

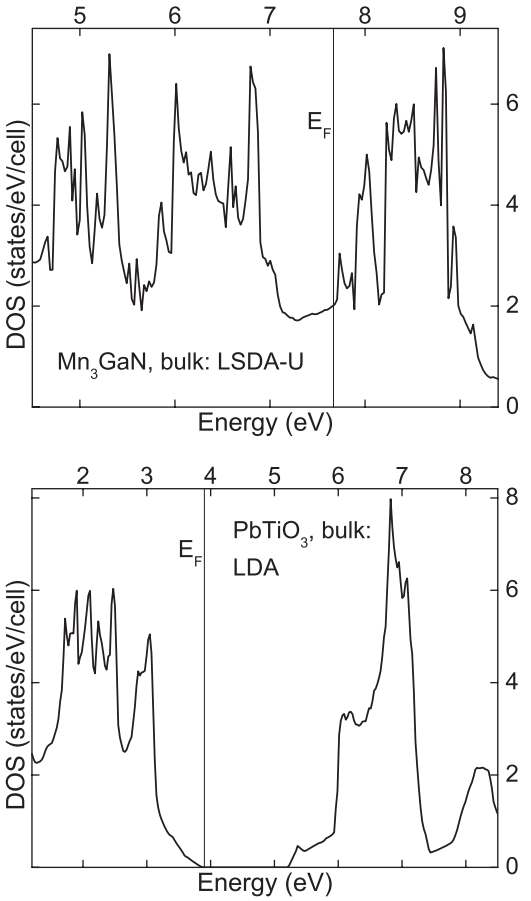

FIG. 5. Densities of states for bulk Mn_3GaN (top panel) and $PbTiO_3$ (bottom panel).

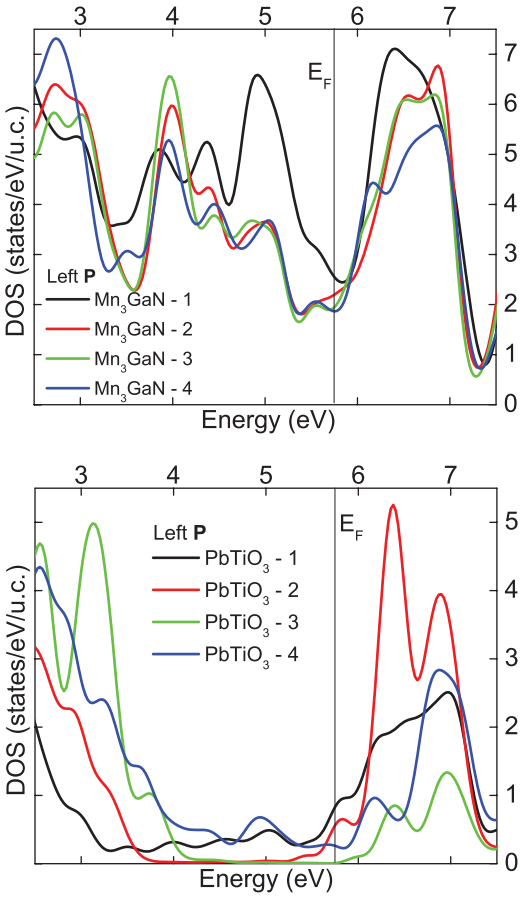

FIG. 6. (Color online) Unit cell (u.c.) resolved densities of states for Mn_3GaN (top panel) and $PbTiO_3$ (bottom panel) in the heterostructure for left **P**. Numbering of the cells is consistent with the one described in Sec. IV.

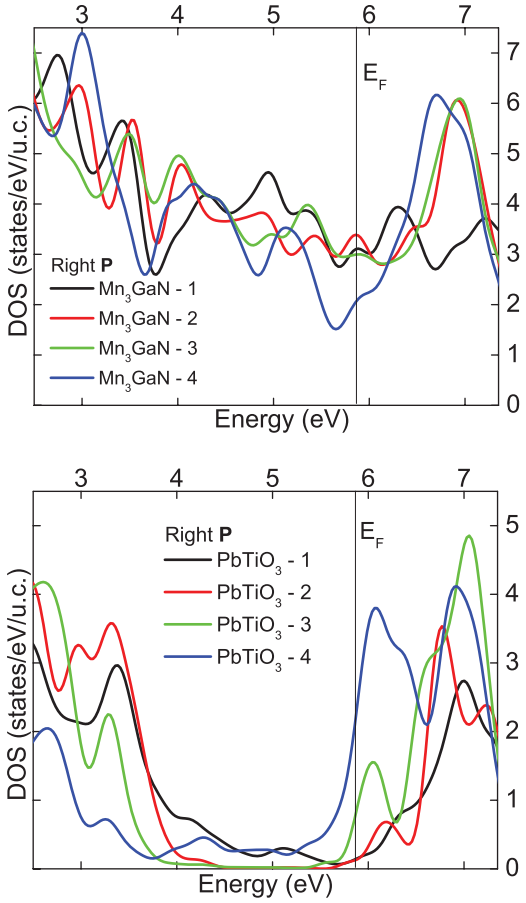

FIG. 7. (Color online) Unit cell resolved densities of states for Mn_3GaN (top panel) and $PbTiO_3$ (bottom panel) in the heterostructure for right **P**. Numbering of the cells is consistent with the one described in Sec. IV.

Figure 6 shows unit cell resolved DOS of Mn_3GaN (top panel) and $PbTiO_3$ (bottom panel) in the heterostructure when FE polarization points left, while Fig. 7 shows DOS in the heterostructure with FE polarization pointing right. The numbering of the cells is consistent with the one described in Sec. IV. Comparison of Fig. 5 with Figs. 6 and 7 shows that DOS in the heterostructure is largely distorted compared with the DOS in the bulk for both Mn_3GaN and $PbTiO_3$. In particular, overlap of the orbitals at both TiO_2/Mn_2N and PbO/GaMn iterfaces results in additional states in the energy gap of $PbTiO_3$. This is evident from bottom panels of Figs. 6 and 7; the nonzero states in the gap are due to interfacial unit cells of $PbTiO_3$ (black line corresponding to the $PbTiO_3$ unit cell at the TiO_2/Mn_2N, while blue line to the $PbTiO_3$ unit cell at the PbO/GaMn interfaces). The noninterfacial unit cells of $PbTiO_3$ in the heterostructure are mostly insulating (see red and green lines at the bottom panels of Figs. 6 and 7). The small nonzero values at the Fermi level are probably coming from broadening of the states and some effect of incomplete basis. The insulating nature is quite obvious from the shift of DOS of cells. The DOS curves are shifted with respect to each other to the higher energy (from *1* to *4*) in case of left **P**, and in opposite direction in case of right **P** because of the electric field present due to polarization. If $PbTiO_3$ in the heterostructure would become metallic in all cells, this shift would be largely screened by conduction electrons.

Mn_3GaN DOS in the heterostructure also undergoes distortion in the heterostructure compared with the bulk (compare top panel of the Fig. 5 with the top panels of the Figs. 6 and 7). For both left and right **P**, DOS of the Mn_3GaN at the PbO/GaMn interface is higher than at the TiO_2/Mn_2N interface (compare black and blue lines at top panels of Figs. 6 and 7). This is consistent with our result that the larger contribution to the induced magnetization comes from the PbO/GaMn interface (see Fig. 4).

VI. CONCLUSIONS

In conclusion, we have demonstrated a mechanism to electrically control the magnetic properties of thin-film layered ferroelectric/piezomagnetic heterostructures (in particular $PbTiO_3/Mn_3GaN$). The magnetization induced in the multilayer is due to the lowering of the Γ^{5g} magnetic symmetry of Mn_3GaN caused by the interfacial strain and FE displacements. The magnetization of the heterostructure can be

controlled by an external electric field by switching the direction of FE polarization. Switching of the polarization changes the magnetization by more than 50%. The FE/PzM interface magnetization shows strong dependence on the direction of the FE polarization. In principle, the ME mechanism described in this work may be used for practical applications, such as in magnetic switches. Therefore we hope that our results will stimulate experimental work on the PzM/FE layered thin-film heterostructures.

ACKNOWLEDGMENTS

P.L. thanks Evgeny Y. Tsymbal for helpful discussions. K.D.B. acknowledges support from the Research Corporation through the Cottrell Scholar Award. This work was supported by the National Science Foundation through Nebraska MRSEC and EPSCoR (Grant Nos. DMR-0906443, DMR-0820521, and EPS-1010674) and the Nanoelectronics Research Initiative. Computations were performed utilizing the Holland Computing Center of the University of Nebraska.

[1] L. D. Landau and E. M. Lifshitz, *Electrodynamics of Continuous Media* (Pergamon, Oxford, 1984).
[2] T. Kimura, T. Goto, H. Shintani, K. Ishizaka, T. Arima, and Y. Tokura, Nature (London) **426**, 55 (2003).
[3] R. Ramesh and N. A. Spaldin, Nat. Mater. **6**, 21 (2007).
[4] C.-G. Duan, S. S. Jaswal, and E. Y. Tsymbal, Phys. Rev. Lett. **97**, 047201 (2006).
[5] M. K. Niranjan, J. P. Velev, C.-G. Duan, S. S. Jaswal, and E. Y. Tsymbal, Phys. Rev. B **78**, 104405 (2008).
[6] J. M. Rondinelli, M. Stengel, and N. Spaldin, Nat. Nanotech. **3**, 46 (2008).
[7] S. Zhang, Phys. Rev. Lett. **83**, 640 (1999).
[8] M. Weisheit, S. Fähler, A. Marty, Y. Souche, C. Poinsignon, and D. Givord, Science **315**, 349 (2007).
[9] M. K. Niranjan, J. D. Burton, J. P. Velev, S. S. Jaswal, and E. Y. Tsymbal, Appl. Phys. Lett. **95**, 052501 (2009).
[10] I. V. Ovchinnikov and K. L. Wang, Phys. Rev. B **78**, 012405 (2008).
[11] Y. Sun, J. D. Burton, and E. Y. Tsymbal, Phys. Rev. B **81**, 064413 (2010).
[12] K. Takenaka and H. Takagi, Appl. Phys. Lett. **87**, 261902 (2005).
[13] E. O. Chi, Solid State Commun. **120**, 307 (2001).
[14] K. Kamishima, T. Goto, H. Nakagawa, N. Miura, M. Ohashi, N. Mori, T. Sasaki, and T. Kanomata, Phys. Rev. B **63**, 024426 (2000).
[15] P. Lukashev, R. F. Sabirianov, and K. D. Belashchenko, Phys. Rev. B **78**, 184414 (2008).
[16] P. Lukashev and R. F. Sabirianov, Phys. Rev. B **82**, 094417 (2010).
[17] E. F. Bertaut, D. Fruchart, J. P. Bouchaud, and R. Fruchart, Solid State Commun. **6**, 251 (1968).
[18] P. E. Blöchl, Phys. Rev. B **50**, 17953 (1994).
[19] G. Kresse and D. Joubert, Phys. Rev. B **59**, 1758 (1999).
[20] M. Methfessel and A. T. Paxton, Phys. Rev. B **40**, 3616 (1989).
[21] Z. Wu, R. E. Cohen, and D. J. Singh, Phys. Rev. B **70**, 104112 (2004).
[22] Y. Umeno, B. Meyer, C. Elsasser, and P. Gumbsch, Phys. Rev. B **74**, 060101(R) (2006).
[23] D. I. Bilc, R. Orlando, R. Shaltaf, G. M. Rignanese, J. Iniguez, and P. Ghosez, Phys. Rev. B **77**, 165107 (2008).
[24] Z. Wu and R. E. Cohen, Phys. Rev. B **73**, 235116 (2006).
[25] J. P. Perdew, K. Burke, and M. Ernzerhof, Phys. Rev. Lett. **77**, 3865 (1996).
[26] A. I. Liechtenstein, V. I. Anisimov, and J. Zaanen, Phys. Rev. B **52**, R5467 (1995).
[27] The corresponding GGA values are $a = 3.84$ Å, $c/a = 1.24$, Ti-O displacement equals to 0.43 Å, and Pb-O displacement equals to 0.71 Å.